nature medicine

Inhibiting Stat3 signaling in the hematopoietic system elicits multicomponent antitumor immunity

Marcin Kortylewski[1,4], Maciej Kujawski[1,4], Tianhong Wang[2], Sheng Wei[1], Shumin Zhang[1], Shari Pilon-Thomas[1], Guilian Niu[1], Heidi Kay[3], James Mulé[1], William G Kerr[1], Richard Jove[1,4], Drew Pardoll[2] & Hua Yu[1,4]

The immune system can act as an extrinsic suppressor of tumors. Therefore, tumor progression depends in part on mechanisms that downmodulate intrinsic immune surveillance. Identifying these inhibitory pathways may provide promising targets to enhance antitumor immunity. Here, we show that Stat3 is constitutively activated in diverse tumor-infiltrating immune cells, and ablating *Stat3* in hematopoietic cells triggers an intrinsic immune-surveillance system that inhibits tumor growth and metastasis. We observed a markedly enhanced function of dendritic cells, T cells, natural killer (NK) cells and neutrophils in tumor-bearing mice with *Stat3*$^{-/-}$ hematopoietic cells, and showed that tumor regression requires immune cells. Targeting Stat3 with a small-molecule drug induces T cell– and NK cell–dependent growth inhibition of established tumors otherwise resistant to direct killing by the inhibitor. Our findings show that Stat3 signaling restrains natural tumor immune surveillance and that inhibiting hematopoietic Stat3 in tumor-bearing hosts elicits multicomponent therapeutic antitumor immunity.

Recent studies suggest a crucial role of immune cells in suppressing tumor emergence and sculpting immunogenic phenotypes of tumors (reviewed in ref. 1). It has also been shown that elements of the tumor microenvironment can promote immune tolerance, at least in part, by bone marrow–derived dendritic cells (DCs)[2–5]. Indeed, although the requirement for DCs in generating T-cell immunity is well established[6], DCs are immature and dysfunctional both in individuals with cancer and in tumor-bearing animals[7,8]. Evidence has been accumulating that oncogenic signaling contributes to tumor immune evasion by inhibiting DC maturation[9–11]. For example, we recently showed that signal transducer and activator of transcription 3 (Stat3), which is frequently activated in diverse cancers by common oncogenic pathways, mediates immune suppression by inhibiting expression of proinflammatory cytokines and chemokines necessary for DC activation[11]. Moreover, tumor Stat3 activity promotes production of multiple factors, among them vascular endothelial growth factor (VEGF) and interleukin (IL)-10, that activate Stat3 signaling and inhibit functional DC maturation in culture[11]. Inhibition of Stat3 activity in DC progenitors has also been shown to reduce accumulation of immature DCs by tumor-derived factors *in vitro*[12]. Furthermore, macrophages devoid of Stat3 signaling do not efficiently induce T-cell anergy, supporting a negative regulatory role of Stat3 in antigen-presenting cells[13].

These findings suggest that Stat3 inhibition could potentially restore DC functions in tumor-bearing hosts. But a recent study showed that DC number is markedly reduced in mice with congenital *Stat3*$^{-/-}$ hematopoietic cells[14], implying that targeting Stat3 in hematopoietic cells *in vivo* might negatively affect DC function and, therefore, antitumor immune responses. We sought to directly determine the role of hematopoietic Stat3 signaling on immune surveillance of tumors and investigate how inhibiting Stat3 in host immune cells *in vivo* might affect the function of various cell subsets and their ability to engage in antitumor immune responses. To bypass the requirement of Stat3 during embryogenesis[15] and to model a therapeutically relevant setting for individuals with cancer, we tested the effects of induced *Stat3* ablation in hematopoietic cells in adult mice before and after tumor establishment. Our data show that Stat3 is constitutively activated in tumor-infiltrating immune cells. Ablation of *Stat3* in hematopoietic cells in adult animals does not reduce DC numbers, but rather enhances DC maturation in tumor-bearing mice. T cells, natural killer (NK) cells and neutrophils in tumor-bearing mice with *Stat3*$^{-/-}$ hematopoietic system show enhanced antitumor activity. Ablating *Stat3* in multiple hematopoietic elements ultimately results in immune cell–mediated antitumor responses. Blocking Stat3 signaling with a small-molecule drug *in vivo* induces immune-mediated antitumor effects. These findings suggest that Stat3 is a key negative regulator of tumor immune surveillance and that it can be manipulated to augment innate and adaptive immune responsiveness to tumors.

RESULTS

Effects of *Stat3* ablation in DCs in adult mice

Using the *Mx1-Cre-lox*P system, ablation of *Stat3* in hematopoietic cells is inducible in adult mice, overcoming the requirement of Stat3

[1]H. Lee Moffitt Cancer Center and Research Institute, 12902 Magnolia Drive, Tampa, Florida 33612, USA. [2]Sidney Kimmel Cancer Center, Johns Hopkins University School of Medicine, 1650 Orleans Street, Baltimore, Maryland 21231, USA. [3]College of Public Health, University of South Florida, 13201 Bruce B. Downs Boulevard, Tampa, Florida 33612, USA. [4]Present address: City of Hope National Medical Center, 1500 Duarte Road, Duarte, California 91010, USA. Correspondence should be addressed to D.P. (dmpardol@jhmi.edu) or H.Y. (hyu@coh.org).

Received 28 June; accepted 13 October; published online 20 November 2005; doi:10.1038/nm1325

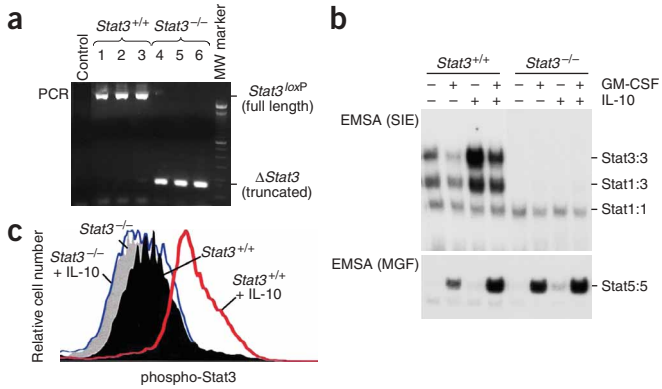

Figure 1 Inducing *Stat3* ablation in hematopoietic cells of adult mice. (**a**) PCR analysis of genomic DNA from bone marrow after poly(I:C) treatment with primer sets that distinguish full-length $Stat3^{loxP}$ and *Stat3*-deleted alleles. (**b**) EMSA confirmed lack of Stat3-DNA binding activity in the $Stat3^{-/-}$ bone marrow cells. SIE is a DNA probe for detecting Stat3 and Stat1 DNA-binding activity, whereas MGF detects Stat5-DNA binding. Positions of Stat homo- and heterodimers are indicated. (**c**) Intracellular flow cytometric analysis using an antibody to detect tyrosine-phosphorylated Stat3 (phospho-Stat3) shows absence of activated Stat3 in $Stat3^{-/-}$ DCs. $CD11c^+$ DCs purified from spleens of $Stat3^{+/+}$ and $Stat3^{-/-}$ mice were stimulated with IL-10, followed by intracellular staining with phospho-Stat3–specific antibody.

in embryogenesis[16,17]. Injection of poly(I:C) into mice carrying the *Mx1-Cre* transgene (*Cre*) and *Stat3* alleles flanked by *lox*P sites ($Stat3^{loxP/loxP}$) led to effective *Stat3* deletion in bone marrow cells, as determined by a PCR-based genotyping assay[18] (**Fig. 1a**), further confirmed by lack of Stat3-DNA binding and phosphorylated Stat3 even after IL-10 stimulation (**Fig. 1b**,**c**). Results from flow cytometric analysis of splenic DCs showed that *Stat3* ablation in hematopoietic cells of adult mice did not reduce the number of $CD11c^+$ DCs over a 4-week period (**Fig. 2a**). Because poly(I:C) is a Toll-like receptor 3 ligand that stimulates interferon (IFN)-α production and activates DCs, there exists the potential that inflammatory responses associated with poly(I:C) treatment might obscure the functional effects resulting from *Stat3* deletion. The effects of poly(I:C) on DCs and other immune cells are confined to the 48 h of treatment (**Supplementary Fig. 1** online). Thus, the immunologic and tumor protection analyses in this study were performed ≥5 d after completion of poly(I:C) treatment in order to focus specifically on the effects of *Stat3* ablation.

We next evaluated how *Stat3* deletion might affect DC activation. Although splenic DCs from tumor-bearing $Stat3^{+/+}$ and hematopoietically *Stat3*-ablated ($Stat3^{-/-}$) mice did not produce IL-12 spontaneously (data not shown), those from $Stat3^{-/-}$ mice expressed higher levels of IL-12 upon *ex vivo* stimulation with lipopolysaccharide (**Fig. 2b**). Moreover, splenic DCs isolated from $Stat3^{-/-}$ mice bearing larger tumors showed enhanced ability to present antigen and activate antigen-specific $CD4^+$ T cells *ex vivo* (**Fig. 2b**). Recent work has focused attention on tumor-infiltrating immune cells as a more direct means of assessing effects of tumor on its immunologic microenvironment[19–23]. We therefore isolated tumor-infiltrating DCs from control and $Stat3^{-/-}$ mice and analyzed expression of relevant DC activation molecules. Flow cytometric analysis after staining with antibody specific for phosphorylated Stat3 showed that Stat3 is

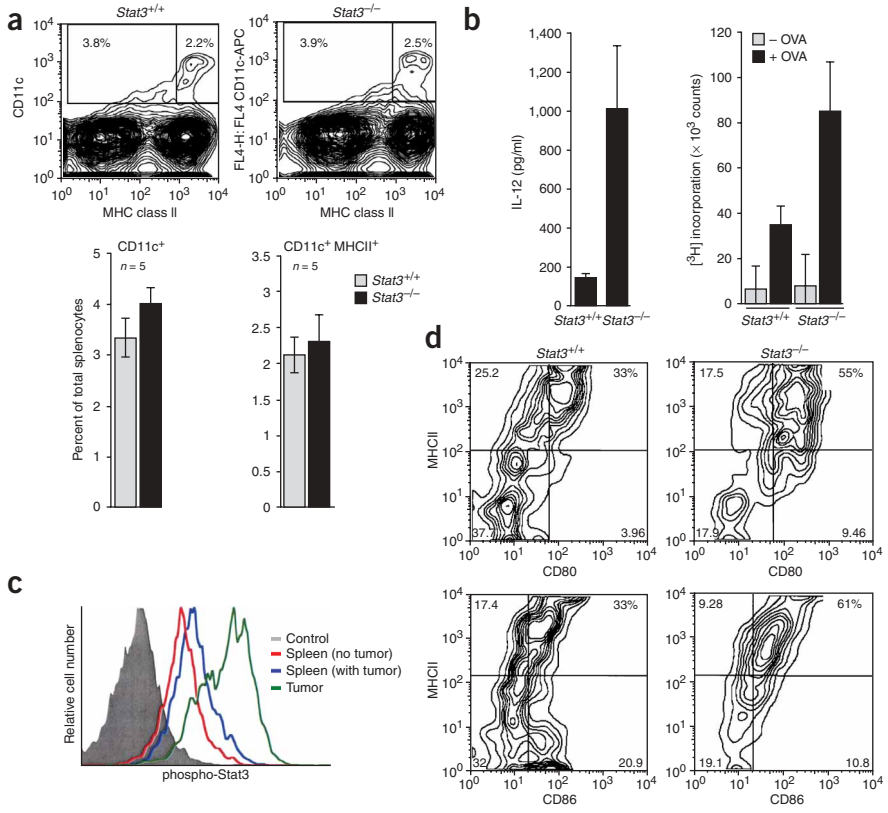

Figure 2 Effects of *Stat3* ablation on DCs. (**a**) Total number of splenic DCs from $Stat3^{-/-}$ mice is not reduced as compared to $Stat3^{+/+}$ in tumor bearing mice. Top, representative analysis of total splenocytes by flow cytometry. Shown are the percentages of $CD11c^+$ and $CD11c^+MHC\ II^{+\ low\ or\ high}$ subsets. Bottom, data from FACS are presented as means ± s.d.; $n = 5$. (**b**) IL-12 ELISA of $CD11c^+$ DCs purified from spleens of tumor-bearing $Stat3^{+/+}$ and $Stat3^{-/-}$ mice after lipopolysaccharide stimulation (left panel). Proliferation of OTII $CD4^+$ T cells stimulated by $Stat3^{+/+}$ and $Stat3^{-/-}$ DCs ± OVA (right panel). Data are shown as means ± s.d.; $n = 3$. (**c**) Stat3 is constitutively activated in tumor-infiltrating DCs as determined by intracellular staining with antibody to phosphorylated Stat3 (phospho-Stat3), followed by flow cytometry. Representative results of three independent experiments with three to four mice per group are shown. (**d**) Percentages of $MHCII^{hi}CD80^{hi}$ or $MHCII^{hi}CD86^{hi}$ tumor-infiltrating $CD11c^+$ DCs are higher in $Stat3^{-/-}$ mice. Shown are representative results of FACS analysis from one of three independent experiments with four to six mice per group.

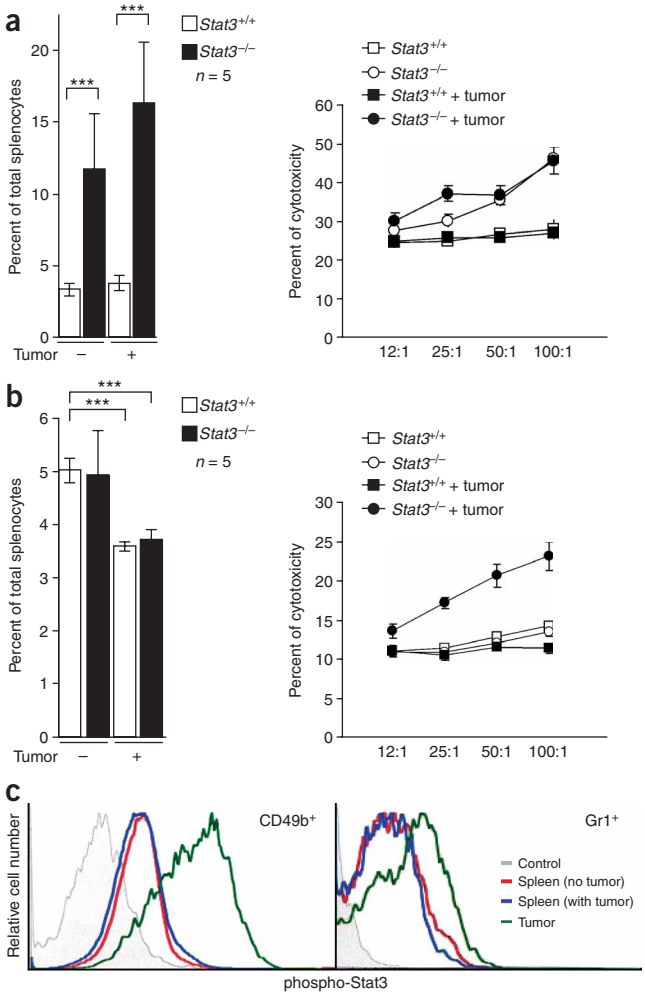

Figure 3 Role of Stat3 signaling in neutrophils and NK cells. (**a**) Number of neutrophils from *Stat3*$^{-/-}$ mice is higher, and *Stat3*$^{-/-}$ neutrophils have stronger cytotoxicity than those from *Stat3*$^{+/+}$ mice. FACS analysis of neutrophils (Gr1^{+}CD11b^{+}) from *Stat3*$^{+/+}$ and *Stat3*$^{-/-}$ mice challenged with B16 tumor (left). Shown are the means ± s.d.; $n = 5$. ***$P < 0.001$. ^{51}Cr-release assay with neutrophils: FcγR^{+} mouse mastocytoma (P815) cells are used as targets (right). Shown are representative results from one of three independent experiments done in triplicates; means ± SD. Two mice were used for each experiment. (**b**) NK cells from tumor-bearing *Stat3*$^{-/-}$ mice showed enhanced cytotoxicity. Splenic NK cells from *Stat3*$^{+/+}$ and *Stat3*$^{-/-}$ mice with and without B16 tumor as in **a** were analyzed by FACS using CD49b-specific antibody (left). Shown are the means ± s.d.; $n = 5$. ***$P < 0.001$. NK cytotoxicity was assessed in ^{51}Cr-release assay using YAC-1 cells as targets (right). Shown are the representative results from one of three independent experiments done in triplicate as in **a**. (**c**) Tumor-infiltrating NK cells (CD49b^{+}) and granulocytes (Gr1^{+}) from wild-type mice showed increased phospho-Stat3 compared with their splenic counterparts. Shown are FACS analyses after intracellular staining with antibody to phospho-Stat3. The data presented were confirmed by two additional experiments.

constitutively activated in tumor-infiltrating DCs (**Fig. 2c**). Furthermore, examination of tumor-infiltrating DCs showed that expression of major histocompatibility complex (MHC) class II, CD80 and CD86 is considerably increased in *Stat3*$^{-/-}$ mice when compared to those from *Stat3*$^{+/+}$ mice (**Fig. 2d**). These results support the notion that Stat3 activation is an important contributor to the impaired activation state of tumor-infiltrating DCs. We further analyzed subsets of tumor-infiltrating DCs in both *Stat3*$^{+/+}$ and *Stat3*$^{-/-}$ mice. Tumor-infiltrating DCs were essentially all CD8^{-} in both *Stat3*$^{+/+}$ and *Stat3*$^{-/-}$ mice (**Supplementary Fig. 2** online). The percentage of B220^{+} plasmacytoid DCs was higher in tumor than in spleen, and a decrease in tumor-infiltrating B220^{+} plasmacytoid DCs in *Stat3*$^{-/-}$ mice was detected (**Supplementary Fig. 2** online). Notably, plasmacytoid DCs are thought to be involved in tolerogenic functions through generation of regulatory T cells[24].

Stat3 signaling and antitumor innate immunity

Innate immunity has an active role in immune surveillance as well as induced antitumor effects[1,25,26]. Because granulocytes can contribute to tumor-cell killing and tumor regression[27,28], we investigated how *Stat3* deficiency might affect their function. In agreement with a recent study[17], induction of *Stat3* deletion considerably increased the number of splenic granulocytic lineage cells (**Fig. 3a**). Analysis of neutrophil cytolytic activity in a ^{51}Cr-release assay using FcγR^{+} mouse mastocytoma (P815) cells as targets indicated that reduced Stat3 signaling in neutrophils enhances their cytolytic activity against target tumor cells, regardless of whether they were isolated from tumor-free or tumor-bearing mice (**Fig. 3a**).

As NK cells are important cytolytic effectors against tumors[29], we investigated whether blocking Stat3 in hematopoietic cells might affect NK-cell numbers and their ability to kill target cells. Immunostaining splenocytes from control or B16 tumor-bearing mice using a pan-NK marker, CD49b, indicated no significant change in the number of NK cells between *Stat3*$^{+/+}$ and hematopoietically *Stat3*-ablated mice (**Fig. 3b**). But, in the presence of tumor, NK-cell numbers were decreased by about 25% in both groups. We assessed splenic NK-cell cytolytic activity using ^{51}Cr-labeled YAC-1 cells as targets. The cytolytic activity of NK cells isolated from tumor-free mice did not differ between poly(I:C)-treated *Stat3*$^{loxP/loxP}$ and *Mx1-Cre-Stat3*$^{loxP/loxP}$ mice. In contrast, after tumor challenge, NK cells from *Stat3*$^{-/-}$ mice showed enhanced cytolytic activity (**Fig. 3b**). Analysis of phosphorylated Stat3 by flow cytometry showed that Stat3 was also constitutively activated in tumor-infiltrating NK cells and neutrophils (**Fig. 3c**). Many tumor-associated factors, including IL-10, VEGF and IL-6, are activators of Stat3, and IL-10 is abundantly produced by macrophages in mice bearing MB49 tumors[30]. Flow cytometry and electrophoretic mobility shift assay (EMSA) indicated that IL-10 activates Stat3 in NK cells (CD49b^{+}CD3^{-}) and granulocytes (Gr1^{+}; **Supplementary Fig. 3** online). Furthermore, our data showed that FasL expression was increased in *Stat3*$^{-/-}$ Gr1^{+}CD11b^{+} neutrophils (**Supplementary Fig. 4** online). Upregulation of FasL has been associated with increased cytotoxicity of neutrophils, and an inhibitory role of Stat3 on FasL expression in tumor cells has been previously reported[31].

The findings of increased function of purified *Stat3*$^{-/-}$ NK cells and neutrophils from tumor-bearing mice together with an increase in Stat3 activity directly within these populations in tumor indicates that the role of Stat3 signaling in downregulating function of these cell types is at least, in part, cell intrinsic. Given the complex intercellular interactions that occur *in vivo* among different immune-cell populations, amplifying cell-extrinsic affects are also a possibility.

T-cell responses in hematopoietically *Stat3*$^{-/-}$ mice

Although ablation of *Stat3* alleles in bone marrow cells led to a reduction of absolute numbers of T cells in tumor-free mice as previously reported[17], we observed no difference in the numbers of

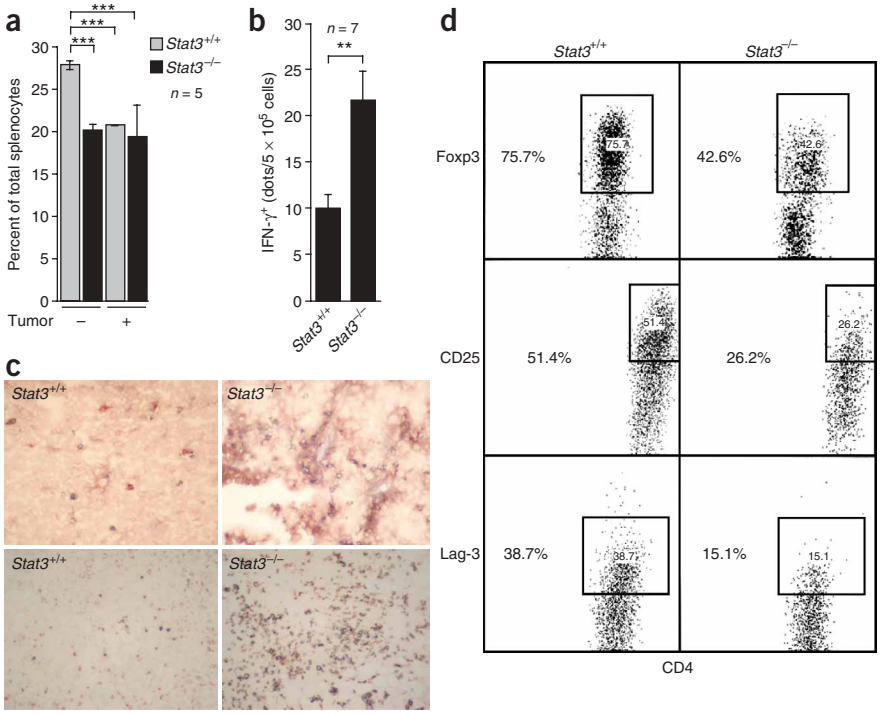

Figure 4 Characterization of T cells from tumor bearing mice with Stat3$^{-/-}$ hematopoietic system. (**a**) Percentage of T cells (CD3$^+$) in spleens of tumor-free and B16 tumor-bearing mice with and without *Stat3* in their hematopoietic system as shown by flow cytometry. Shown are the means ± s.d.; $n = 5$, $P < 0.001$. (**b**) T cells from B16 tumor-bearing mice with *Stat3*$^{-/-}$ hematopoietic cells were able to mount stronger responses against an endogenous B16 tumor antigen than their *Stat3*$^{+/+}$ counterparts, as assessed by IFN-γ ELISPOT. Data shown are mean numbers of p15E-specific IFN-γ–producing spots from seven to nine separate mice per group analyzed individually. $^{**}P = 0.0092$. (**c**) T cells in mice with *Stat3*$^{-/-}$ hematopoietic cells infiltrate tumors more efficiently. Immunohistochemical analysis of B16 (top) and MB49 (bottom) tumor tissue sections prepared from *Stat3*$^{+/+}$ and *Stat3*$^{-/-}$ mice. Red indicates CD8 staining; blue indicates CD4 staining. (**d**) The percentages of tumor-infiltrating T_{reg} cells from *Stat3*$^{-/-}$ mice are reduced, as shown in B16 tumors. The surface expression of CD25 and Lag-3 or the intracellular levels of Foxp3 was evaluated in tumor-infiltrating CD4$^+$ T cells by flow cytometry. Shown are percentages of double-positive cells, representative of three independent experiments.

T cells in the tumor-bearing *Stat3*$^{+/+}$ versus *Stat3*$^{-/-}$ mice (**Fig. 4a**). To address whether T cells isolated from *Stat3*$^{-/-}$ mice could mount tumor antigen–specific immune responses, we treated *Stat3*$^{loxP/loxP}$ and *Mx1-Cre-Stat3*$^{loxP/loxP}$ mice with poly(I:C), followed by B16 tumor challenge. Two weeks after tumor challenge, we analyzed splenocytes for T-cell response to p15E, an endogenous retroviral gene product of the B16 tumor. IFN-γ ELISPOT assay indicated that T cells from *Stat3*$^{-/-}$ mice mounted stronger responses against tumor antigen than their *Stat3*$^{+/+}$ counterparts (**Fig. 4b**).

Because the ability of T cells to infiltrate tumors is considered crucial for induction of tumor regression[32,33], we determined whether T cells from *Stat3*$^{-/-}$ mice could efficiently infiltrate tumors. Immunohistochemical staining of B16 and MB49 mouse tumors showed considerably higher infiltration by T lymphocytes in tumor tissues from *Stat3*$^{-/-}$ mice (**Fig. 4c**). As eradication of tumors, including B16 tumors, is thought to be inhibited by T regulatory (T_{reg}) cells[23,34], we examined whether *Stat3* deficiency in hematopoietic cells might affect tumor-infiltrating T_{reg} cells. Indeed, the proportions of tumor-infiltrating CD4$^+$ T cells expressing T_{reg} markers (CD25, Foxp3 and Lag-3) in *Stat3*$^{-/-}$ mice were considerably reduced (**Fig. 4d**). Changes in tumor-infiltrating T_{reg} cells might be the result of *Stat3* ablation in T cells or indirect effects influenced by Stat3 signaling in other immune cells. Although PCR analyses indicate that *Stat3* is deleted in bone marrow cells from poly(I:C)-treated *Mx1-Cre-Stat3*$^{loxP/loxP}$ mice, *Stat3* is not efficiently ablated in their thymus (data not shown).

Stat3 in hematopoietic cells and antitumor immunity

The ability to induce hematopoietic *Stat3* ablation in our system allows us to determine how Stat3 signaling in hematopoietic cells ultimately affects tumor growth independent of Stat3 activity within tumor cells. We first examined whether ablating *Stat3* in hematopoietic cells might affect tumor establishment. Ablating *Stat3* alleles in hematopoietic cells before subcutaneous tumor challenge significantly inhibited B16(F10) tumor growth (**Fig. 5a**). Some of the MB49 tumors initially grew in the *Stat3*-ablated mice, but they eventually all regressed (**Fig. 5b**). Because essentially all of the immune effects of poly(I:C) treatment have completely subsided by 48 h after treatment (**Supplementary Fig. 1** online), we performed tumor challenge experiments 5 d after the last poly(I:C) treatment, and all control groups included poly(I:C) injection to minimize potential antitumor effects resulting from poly(I:C) itself.

Deletion of *Stat3* in the *Mx1-Cre-Stat3*$^{loxP/loxP}$ also occurs, albeit to a lesser degree, in some tissues other than those of hematopoietic lineage[16,35]. To prove that the observed antitumor effects were contributed by *Stat3* ablation in the hematopoietic compartment, we reconstituted lethally irradiated wild-type recipients with *Stat3*$^{+/+}$ or *Stat3*$^{-/-}$ bone marrow. We challenged mice with engrafted *Stat3*$^{+/+}$ or *Stat3*$^{-/-}$ bone marrow with MB49 tumors 2 months after bone marrow transplant (**Fig. 5c**). We observed growth inhibition followed by complete rejection of tumors in mice with reconstituted *Stat3*$^{-/-}$ bone marrow, whereas tumors in *Stat3*$^{+/+}$ mice grew progressively. These results confirmed that loss of Stat3 in the hematopoietic system mediates the observed antitumor effects. We next determined whether blocking Stat3 signaling in immune cells would have therapeutic antitumor effects. We first challenged *Stat3*$^{loxP/loxP}$ and *Cre-Stat3*$^{loxP/loxP}$ mice with B16(F10) tumor cells. When tumors became palpable, we administered poly(I:C) to both groups. Ablating the *Stat3* alleles in hematopoietic cells led to significant growth inhibition of established B16(F10) tumors (**Fig. 5d**). Moreover, ablation of the *Stat3* alleles in hematopoietic cells induced regression and, in most cases, eradication of established MB49 tumors (**Fig. 5e**). We observed no effect on tumor growth after poly(I:C) treatment of *Stat3*$^{+/+}$ mice, confirming the role of Stat3 signaling in the observed therapeutic antitumor response.

We further determined whether T-cell responses are involved in the observed antitumor effects mediated by inhibiting Stat3 signaling in immune cells. We injected poly(I:C)-treated *Cre-Stat3*$^{loxP/loxP}$ mice with either rat IgG or CD4- and CD8-specific antibodies, which depleted 99% of T cells as confirmed by flow cytometry (data not shown), and challenged mice with MB49 tumor cells. Although

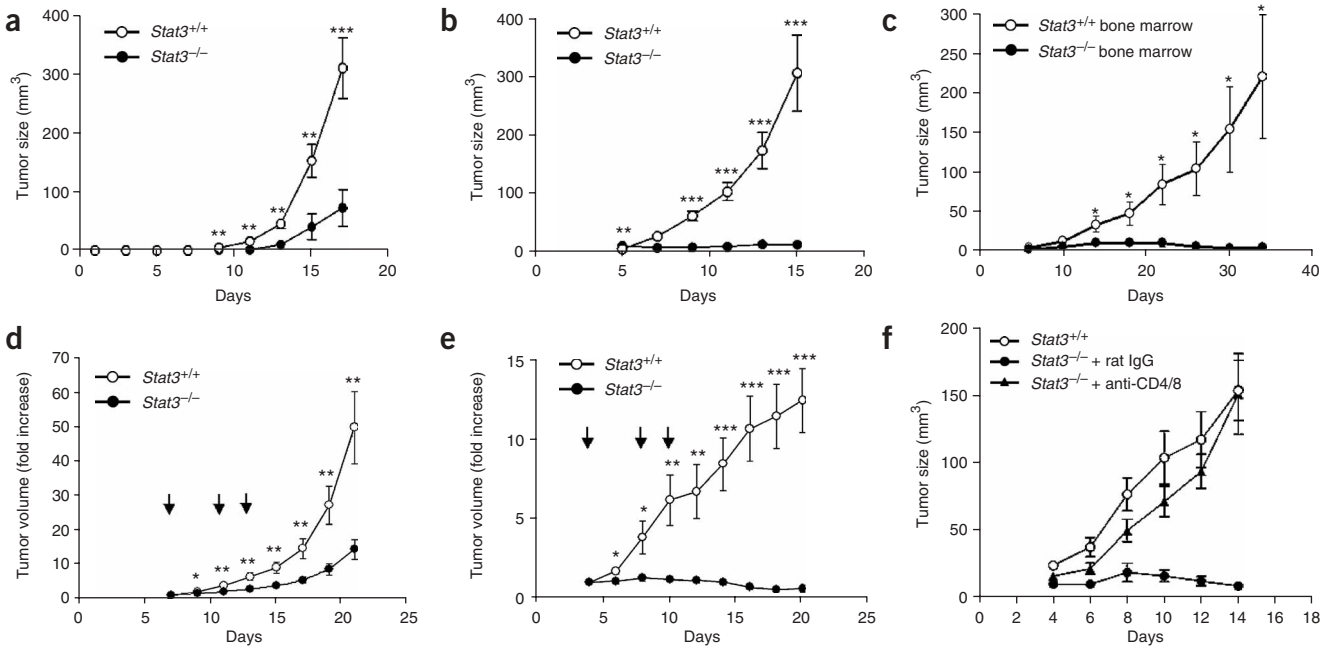

Figure 5 Ablating Stat3 in hematopoietic cells induces antitumor effects. (**a**) B16 tumor development is significantly inhibited in *Stat3*$^{-/-}$ mice. Shown are the results representative of three independent experiments; $n = 10$ for each experiment. $^{***}P < 0.001$; $^{**}P < 0.01$; $^{*}P < 0.05$. (**b**) MB49 tumor growth is abrogated in mice with *Stat3*$^{-/-}$ hematopoietic cells. Shown are the results representative for two independent experiments; $n = 10$ for each experiment. (**c**) MB49 tumor growth is abolished in mice engrafted with *Stat3*$^{-/-}$ whole bone marrow. Tumor challenge was performed 2 months after transplantation of bone marrow from poly(I:C)-treated *Stat3*$^{loxP/loxP}$ and *Cre-Stat3*$^{loxP/loxP}$ mice, $n = 10$. (**d**) Ablating *Stat3* significantly inhibits established B16 tumor growth. Poly(I:C) was administered to *Stat3*$^{loxP/loxP}$ and *Cre-Stat3*$^{loxP/loxP}$ mice bearing B16 tumors (average diameter, 4 mm) on days indicated by arrow, $n = 12$. (**e**) Ablation of the *Stat3* induced complete regression of established MB49 tumors. Average tumor diameter was 6 mm on the day of initial poly(I:C) treatment, $n = 9$. Shown are the results representing two independent experiments. (**f**) Stat3 blockade-induced antitumor effects require T cells. MB49 tumors were implanted in poly(I:C)-treated *Stat3*$^{loxP/loxP}$ and *Cre-Stat3*$^{loxP/loxP}$ mice as in **b**. *Stat3*$^{-/-}$ mice were injected with a control rat IgG or antibodies to CD4 and CD8, as indicated. Statistical significance of the experiment was tested by one-way ANOVA, $P = 0.0196$, $n = 5$. Data are mean numbers ± s.e.m.

ablation of the *Stat3* alleles in bone marrow cells abrogated MB49 tumor growth as expected, the observed antitumor effects were essentially lost in the absence of CD4$^+$ and CD8$^+$ T cells (**Fig. 5f**). Previous studies indicated that long-term *Stat3* ablation leads to autoimmunity. Our analysis indicated that although *Stat3* ablation–induced antitumor immunity is apparent within a week, there was virtually no evidence of systemic autoimmunity at 4 weeks after induced depletion (**Supplementary Fig. 5** online), suggesting that the antitumor responses induced by *Stat3* ablation are not simply a manifestation of systemic autoimmunity in these mice, but rather a specific effect on intrinsic tumor immune surveillance.

Targeting Stat3 induces antitumor immune responses

We next assessed whether blocking Stat3 with a small-molecule Stat3 inhibitor, CPA-7 (ref. 36), would activate immune cells and induce therapeutic antitumor effects *in vivo* independent of direct effects on the tumor cells themselves. In contrast to B16, MB49 tumor cells are insensitive to CPA-7–induced tumor-cell apoptosis (**Fig. 6a**). It has been shown that CPA-7 disrupts Stat3-DNA binding activity, which is followed, within hours, by a reduction of phosphorylated Stat3 in the treated cells *in vitro*[36]. We showed that CPA-7 inhibits Stat3 but not Stat1 and Stat5 in DC2.4 mouse DC line (**Supplementary Fig. 6** online). Tumor-infiltrating DCs from the mice receiving CPA-7 24 h earlier showed considerably reduced phosphorylated Stat3 compared to vehicle-treated mice (**Fig. 6b**). These tumor-infiltrating DCs also have increased phosphorylated Stat1 (**Fig. 6b**). An increase in Stat1 activity in cultured *Stat3*$^{-/-}$ macrophages has been reported, in keeping with opposing activities often observed between these two Stat proteins[18,37,38]. CPA-7 treatment *in vivo* also led to significant growth inhibition of established MB49 tumors (**Fig. 6c**). In the absence of CD4$^+$ and CD8$^+$ T cells, CPA-7–induced tumor growth inhibition was abrogated, suggesting a direct role for immune cells in the *in vivo* antitumor effects of CPA-7 (**Fig. 6c**).

NK cells may also participate in the antitumor effects of CPA-7, as *in vitro* NK cell activity is increased from tumor-bearing mice treated with CPA-7 (**Fig. 6d**) and NK depletion partially abrogates the *in vivo* antitumor effects of CPA-7 treatment (**Fig. 6e**). These data suggest that targeting Stat3 with small-molecule drugs has the potential to induce therapeutic antitumor responses through activating immune cells regardless of the tumors' direct sensitivity to the inhibitors (**Fig. 6f**). Additional experiments further indicated that blocking Stat3 signaling with a small molecule inhibits tumor metastasis and prolongs survival of tumor bearing mice (**Supplementary Fig. 7** online).

As mentioned above, long-term ablation of *Stat3* in hematopoietic cells is known to cause Crohn disease–like pathology (**Supplementary Fig. 5** online). To determine whether there is indeed a therapeutic window for Stat3-based cancer treatment, we assessed the effects of 3-week CPA-7 treatment on lymphocytes and macrophage infiltration in colons. We observed no such infiltration in tumor-bearing mice treated with CPA-7 over the 3-week treatment period necessary for effective antitumor responses (**Supplementary Fig. 5** online). Moreover, no significant toxicity was detected in mice receiving 4-week CPA-7 treatment (**Supplementary Table 1** online). These results

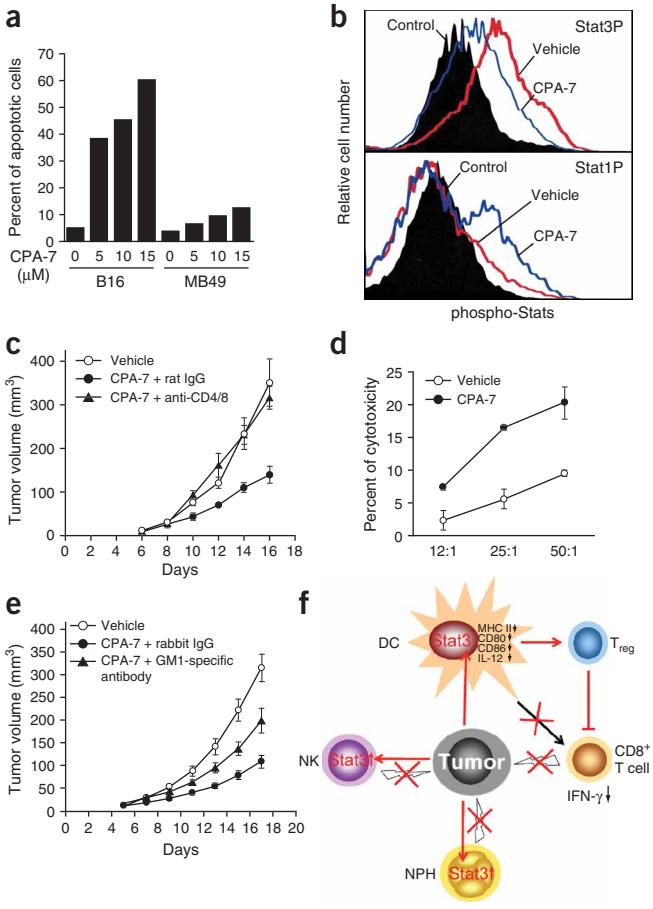

Figure 6 Targeting Stat3 with a small-molecule inhibitor activates antitumor immunity. (**a**) Sensitivity of tumor cells to CPA-7–induced apoptosis *in vitro* as determined by annexin V staining. B16 cells, sensitive to CPA-7–induced apoptosis, served as a positive control. (**b**) Stat3 is activated in tumor-infiltrating DCs, and administering CPA-7 to MB49 tumor-bearing mice reduces Stat3 whereas Stat1 activity was increased. Top panel: Phospho-Stat3 (Stat3P) levels in tumor-infiltrating DCs were assessed 24 h after intravenous injection with vehicle (red line) or CPA-7 (blue line). Control was splenic CD11c$^+$ cells from tumor-free *Stat3*$^{+/+}$ mice. Lower panel: Stat1YP levels in tumor-infiltrating DCs from the same mice as in top panel. (**c**) Blocking Stat3 with CPA-7 inhibits the growth of established MB49 tumors, which is T cell dependent. Mice with tumors (about 6 mm in diameter) received intravenous injections of either vehicle or CPA-7; $P = 0.0088$ (by one-way ANOVA), $n = 6$. (**d**) Targeting Stat3 with CPA-7 activates NK cells in tumor-bearing hosts. Shown is ^{51}Cr-release assay using YAC-1 target cells; $n = 3$. (**e**) Effects of depleting NK cells with antibody to asialo GM1. Mice with established MB49 tumors were treated with vehicle or CPA-7 in combination with control or asialo GM1-specific antibody; $P < 0.0001$ (by one-way ANOVA), $n = 11$. (**f**) Schematic overview on Stat3 as a negative regulator of antitumor immunity and potential target for immunotherapy. Tumor microenvironment induces Stat3 activity in various immune cells. Stat3 activity in tumor-associated NK cells and neutrophils inhibits direct cell cytotoxicity and antitumor innate immune responses. Activation of Stat3 in tumor-infiltrating DCs impedes CD8$^+$ T-cell function, and may contribute to accumulation of tolerogenic T_{reg} cells inside tumors.

suggest that targeting Stat3 can induce immune cell–mediated antitumor effects without systemic autoimmunity.

DISCUSSION

In our inducible *Stat3* knockout mouse model, *Stat3* ablation affected multiple lineages of immune cells, many of which show enhanced antitumor activity when assayed in isolation. *In vivo*, specific alterations in cellular interactions that occur when Stat3 is pharmacologically blocked or genetically ablated lead to potent antitumor responses, irrespective of tumor sensitivity to Stat3 inhibition. Our previous cell-culture studies showed that tumor-derived factors such as VEGF and IL-10 activate Stat3 in DC progenitors, and that blocking Stat3—by either a Stat3 peptide inhibitor or gene ablation—abrogates tumor-induced maturation inhibition *in vitro*[11]. Based on these data, it is probable that Stat3 signaling directly influences DC maturation and activation. Whether *Stat3* deficiency within T cells, neutrophils and NK cells is solely responsible for the enhanced cytolytic activity remains to be further investigated. Nonetheless, our study shows that Stat3 signaling restrains multiple hematopoietically derived elements of innate and adaptive immunity. Moreover, our results show that Stat3 is persistently activated in tumor-infiltrating immune cells and that targeting Stat3 in the hematopoietic system elicits multicomponent therapeutic antitumor immunity.

Stat3 regulates multiple genes crucial for tumor-cell survival and proliferation[39,40]. Targeting Stat3 in tumors with constitutive Stat3 activation causes direct tumor-cell death[40] and growth inhibition *in vivo*[41,42]. Our findings show that inhibiting Stat3 in the hematopoietic system can result in immune cell–mediated antitumor immunity against tumors otherwise insensitive to direct Stat3 inhibition. *Stat3* ablation leads to autoimmune manifestation in the gut[35,43]. We observed marginal immune cell infiltration in colon 4 weeks after hematopoietic *Stat3* ablation, but the antitumor effects of hematopoietic *Stat3* ablation are more rapid, becoming obvious within a week. Thus, there is a considerable therapeutic window of antitumor immunity versus autoimmunity. This therapeutic window is emphasized by our studies showing CPA-7 treatment causes antitumor immune responses without detectable manifestation of autoimmunity within the gut. Inhibiting Stat3 by means other than gene deletion is incomplete and/or intermittent as a result of limited half-life of drugs[11,36], suggesting that molecular targeting of Stat3 allows at least some normal function of Stat3. Targeting Stat3 is expected to affect Stat3 activity most markedly in tumor-infiltrating immune cells, tumor cells and tumor stromal cells, because Stat3 is preferentially activated in these cells compared to their counterparts in normal tissue. We propose that targeting Stat3 in tumor-infiltrating immune cells may block expression of many tumor-associated factors and their corresponding receptor signaling, neutralizing the tumor-induced immunosuppressive microenvironment and thereby contributing to antitumor immunity. In light of immune impairment in individuals with cancer, short-term blockade of Stat3 in a controlled manner—using small-molecule drugs or RNA interference—may reverse immune suppression and activate antitumor immune responses, which could be harnessed to improve the efficacy of immunotherapeutic approaches.

METHODS

Cells lines. We purchased mouse B16 melanoma and YAC-1, P815 target cells, from American Type Culture Collection; MB49 bladder carcinoma and C4 mouse melanoma lines were gifts from T. Ratliff (University of Iowa) and J. Fidler (M.D. Anderson Cancer Center), respectively.

***In vivo* experiments.** Mouse care and experimental procedures were performed under pathogen-free conditions in accordance with established institutional guidance and approved protocols from Institutional Animal Care and Use Committees of University of South Florida and John Hopkins University. We obtained *Mx1-Cre* mice from the Jackson Laboratory and *Stat3*$^{loxP/loxP}$ mice

from S. Akira and K. Takeda (Osaka University). Generation of mice with *Stat3*$^{-/-}$ hematopoietic cells by an inducible *Mx1-Cre* recombinase system has been reported[17,35]. Briefly, we verified deletion of *Stat3* by PCR, using primer sets that distinguish *Stat3*, *Stat3*^{loxP} and *Stat3*-deleted alleles, and by EMSA. For EMSA, we prepared nuclear extracts from *Stat3*$^{+/+}$ and *Stat3*$^{-/-}$ bone marrow cells stimulated for 20 min with IL-10 (10 ng/ml) and/or GM-CSF (20 ng/ml). We performed bone marrow transplantations with whole bone marrow obtained from *Stat3*$^{+/+}$ and *Stat3*$^{-/-}$ donor mice as described previously[44]. For subcutaneous tumor challenge, we injected 5×10^4 B16 or 5×10^5 MB49 tumor cells into 7–8-week-old wild-type mice at 5 d after poly(I:C) treatment, or 2 months after bone marrow transplant. After 3–5 weeks, mice were killed and spleens as well as tumor specimens were harvested. For therapeutic studies, we challenged *Stat3*$^{loxP/loxP}$ or *Cre-Stat3*$^{loxP/loxP}$ mice with either B16 or MB49 tumor cells, followed by poly(I:C) treatments when tumors were at least 3–5 mm in diameter. Because of a male antigen–specific response in female mice by tumor challenge, we carried out MB49 tumor experiments using male mice only.

For CPA-7 treatment, we implanted MB49 tumors into male C57BL/6 mice and allowed the tumors to grow until 5–7 mm in diameter; we gave mice intravenous injections of either vehicle (10% DMSO/PBS) or 5 mg/kg CPA-7 once every 3 d.

Flow cytometry. We prepared single-cell suspensions by mechanic dispersion of spleen or tumor tissues. We preincubated 1×10^6 freshly prepared cells suspended in a mixture of PBS, 2% FCS and 0.1% (wt/vol) sodium azide with FcγIII/IIR-specific antibody to block nonspecific binding and stained the cells with different combinations of fluorochrome-coupled antibodies to CD11c, I-A^b (MHC class II), CD86, CD11b, Gr1, CD49b, CD3, CD25 or Lag-3, or with annexin V (BD Biosciences). We collected fluorescence data on FACSCalibur (Beckton Dickinson) and analyzed them using FlowJo software (Tree Star).

Isolation of tumor-infiltrating immune cell subsets and intracellular staining of signaling molecules. We gently minced freshly excised tumor tissues into small pieces, and incubated them in 400 U/ml of collagenase D (Roche) solution for 30 min at 37 °C. We used cell suspensions filtered through a mesh filter for isolation of various immune cell subsets using specific antibodies in combination with EasySep magnetic nanoparticles from StemCell Technologies. We fixed isolated tumor-infiltrating cells in paraformaldehyde and permeated them in methanol before intracellular staining with antibodies to phosphotyrosine-Stat3 and Stat1 (BD Biosciences) or with Foxp3-specific antibody (eBiosciences). We collected fluorescence data on FACScalibur (Beckton Dickinson) and analyzed them using FlowJo software (Tree Star).

Isolation and functional analysis of splenic DCs. We isolated DCs from mouse spleens essentially as described[45] and purified them using CD11c MACS beads (Miltenyi Biotec). For IL-12 measurement by ELISA (Endogen), we cultured DCs with 100 ng/ml lipopolysaccharide for 18 h to collect supernatants. T-cell proliferation assay with CD4$^+$ T cells purified from OTII mice stimulated was performed as described previously[11].

Immunohistochemistry. We fixed 5-μm sections of the flash-frozen tumor specimens in acetone, stained them with antibodies to CD4 and CD8, and detected them with peroxidase- or alkaline phosphatase–coupled secondary antibodies using NovaRED and Blue Chromogen from Vector as previously described[44].

Cytotoxicity assays. We performed NK cell and neutrophil cytotoxicity assays as previously described[46]. Briefly, we carried out a 4-h ^{51}Cr-release assay using YAC-1 cells or the FcγR$^+$ mouse mastocytoma (P815) cells as targets for enriched NK cells and neutrophils, respectively.

ELISPOT assay. We harvested spleens from mice challenged subcutaneously with 1×10^5 B16 tumor cells 2 weeks earlier. We seeded 5×10^5 splenocytes into each well of a 96-well filtration plate in the presence or absence of 10 μg/ml of p15E peptide and incubated them at 37 °C for 24 h. We detected peptide-specific IFN-γ–positive spots according to the manufacturer's procedure (Cell Sciences), and scanned and quantified them using Immunospot Analyzer from Cellular Technology Ltd.

Statistical analysis. To compare tumor size or surface marker expression between multiple test groups in mouse experiments, we performed a one-way ANOVA followed by Newman-Keuls test. We used unpaired *t*-test to calculate two-tailed *p* value to estimate statistical significance of differences between two treatment groups. Statistically significant *p* values were labeled as follows: $***P < 0.001$; $**P < 0.01$ and $*P < 0.05$. Data were analyzed using Prism software (GraphPad).

Note: Supplementary information is available on the Nature Medicine website.

ACKNOWLEDGMENTS

We would like to thank G. Gao for statistical analyses, C. Muro-Cacho for evaluating immunohistochemical data, K. Nguyen and T. Ghansah for sharing their expertise and L. Lutz for technical assistance. This work was supported by US National Institutes of Health grants (to H.Y.), and by the Dr. Tsai-fan Yu Cancer Research Endowment. Work in D.P.'s lab was supported by grants from the Commonwealth Foundation, Janey Fund, the Seraph Foundation, the Topecers and D. Needle. W.G.K. is the Newman Scholar of the Leukemia and Lymphoma Society. We would also like to thank S. Akira and K. Takeda for *Stat3*^{loxP} mice, and the Pathology Core at the University of South Florida for technical assistance. We also acknowledge dedication of staff members at the animal facilities and flow cytometry cores at both Moffitt Cancer Center and Johns Hopkins Cancer Center.

COMPETING INTERESTS STATEMENT

The authors declare that they have no competing financial interests.

Published online at http://www.nature.com/naturemedicine/
Reprints and permissions information is available online at http://npg.nature.com/reprintsandpermissions/

1. Dunn, G.P., Bruce, A.T., Ikeda, H., Old, L.J. & Schreiber, R.D. Cancer immunoediting: from immunosurveillance to tumor escape. *Nat. Immunol.* **3**, 991–998 (2002).
2. Pardoll, D. Does the immune system see tumors as foreign or self? *Annu. Rev. Immunol.* **21**, 807–839 (2003).
3. Hawiger, D. *et al.* Dendritic cells induce peripheral T cell unresponsiveness under steady state conditions *in vivo*. *J. Exp. Med.* **194**, 769–779 (2001).
4. Sotomayor, E.M. *et al.* Cross-presentation of tumor antigens by bone marrow-derived antigen-presenting cells is the dominant mechanism in the induction of T-cell tolerance during B-cell lymphoma progression. *Blood* **98**, 1070–1077 (2001).
5. Spiotto, M.T. *et al.* Increasing tumor antigen expression overcomes "ignorance" to solid tumors via crosspresentation by bone marrow-derived stromal cells. *Immunity* **17**, 737–747 (2002).
6. Lanzavecchia, A. & Sallusto, F. Regulation of T cell immunity by dendritic cells. *Cell* **106**, 263–266 (2001).
7. Vicari, A.P., Caux, C. & Trinchieri, G. Tumour escape from immune surveillance through dendritic cell inactivation. *Semin. Cancer Biol.* **12**, 33–42 (2002).
8. Almand, B. *et al.* Clinical significance of defective dendritic cell differentiation in cancer. *Clin. Cancer Res.* **6**, 1755–1766 (2000).
9. Ratta, M. *et al.* Dendritic cells are functionally defective in multiple myeloma: the role of interleukin-6. *Blood* **100**, 230–237 (2002).
10. Melani, C., Chiodoni, C., Forni, G. & Colombo, M.P. Myeloid cell expansion elicited by the progression of spontaneous mammary carcinomas in c-erbB-2 transgenic BALB/c mice suppresses immune reactivity. *Blood* **102**, 2138–2145 (2003).
11. Wang, T. *et al.* Regulation of the innate and adaptive immune responses by Stat-3 signaling in tumor cells. *Nat. Med.* **10**, 48–54 (2004).
12. Nefedova, Y. *et al.* Hyperactivation of STAT3 is involved in abnormal differentiation of dendritic cells in cancer. *J. Immunol.* **172**, 464–474 (2004).
13. Cheng, F. *et al.* A critical role for Stat3 signaling in immune tolerance. *Immunity* **19**, 425–436 (2003).
14. Laouar, Y., Welte, T., Fu, X.Y. & Flavell, R.A. STAT3 is required for Flt3L-dependent dendritic cell differentiation. *Immunity* **19**, 903–912 (2003).
15. Takeda, K. *et al.* Targeted disruption of the mouse Stat3 gene leads to early embryonic lethality. *Proc. Natl. Acad. Sci. USA* **94**, 3801–3804 (1997).
16. Kuhn, R., Schwenk, F., Aguet, M. & Rajewsky, K. Inducible gene targeting in mice. *Science* **269**, 1427–1429 (1995).
17. Lee, C.K. *et al.* STAT3 is a negative regulator of granulopoiesis but is not required for G-CSF-dependent differentiation. *Immunity* **17**, 63–72 (2002).
18. Takeda, K. *et al.* Enhanced Th1 activity and development of chronic enterocolitis in mice devoid of Stat3 in macrophages and neutrophils. *Immunity* **10**, 39–49 (1999).
19. Coussens, L.M. & Werb, Z. Inflammation and cancer. *Nature* **420**, 860–867 (2002).
20. Guiducci, C., Vicari, A.P., Sangaletti, S., Trinchieri, G. & Colombo, M.P. Redirecting *in vivo* elicited tumor infiltrating macrophages and dendritic cells towards tumor rejection. *Cancer Res.* **65**, 3437–3446 (2005).
21. Mantovani, A., Sozzani, S., Locati, M., Allavena, P. & Sica, A. Macrophage polarization: tumor-associated macrophages as a paradigm for polarized M2 mononuclear phagocytes. *Trends Immunol.* **23**, 549–555 (2002).

22. Vicari, A.P. *et al.* Reversal of tumor-induced dendritic cell paralysis by CpG immunostimulatory oligonucleotide and anti-interleukin 10 receptor antibody. *J. Exp. Med.* **196**, 541–549 (2002).
23. Yu, P. *et al.* Intratumor depletion of CD4+ cells unmasks tumor immunogenicity leading to the rejection of late-stage tumors. *J. Exp. Med.* **201**, 779–791 (2005).
24. Colonna, M., Trinchieri, G. & Liu, Y.J. Plasmacytoid dendritic cells in immunity. *Nat. Immunol.* **5**, 1219–1226 (2004).
25. Degli-Esposti, M.A. & Smyth, M.J. Close encounters of different kinds: dendritic cells and NK cells take centre stage. *Nat. Rev. Immunol.* **5**, 112–124 (2005).
26. Diefenbach, A., Jamieson, A.M., Liu, S.D., Shastri, N. & Raulet, D.H. Ligands for the murine NKG2D receptor: expression by tumor cells and activation of NK cells and macrophages. *Nat. Immunol.* **1**, 119–126 (2000).
27. Dranoff, G. Cytokines in cancer pathogenesis and cancer therapy. *Nat. Rev. Cancer* **4**, 11–22 (2004).
28. Golumbek, P.T. *et al.* Treatment of established renal cancer by tumor cells engineered to secrete interleukin-4. *Science* **254**, 713–716 (1991).
29. Smyth, M.J. *et al.* Differential tumor surveillance by natural killer (NK) and NKT cells. *J. Exp. Med.* **191**, 661–668 (2000).
30. Halak, B.K., Maguire, H.C., Jr. & Lattime, E.C. Tumor-induced interleukin-10 inhibits type 1 immune responses directed at a tumor antigen as well as a non-tumor antigen present at the tumor site. *Cancer Res.* **59**, 911–917 (1999).
31. Ivanov, V.N. *et al.* Cooperation between STAT3 and c-jun suppresses Fas transcription. *Mol. Cell* **7**, 517–528 (2001).
32. Ho, W.Y., Blattman, J.N., Dossett, M.L., Yee, C. & Greenberg, P.D. Adoptive immunotherapy: engineering T cell responses as biologic weapons for tumor mass destruction. *Cancer Cell* **3**, 431–437 (2003).
33. Spiotto, M.T., Rowley, D.A. & Schreiber, H. Bystander elimination of antigen loss variants in established tumors. *Nat. Med.* **10**, 294–298 (2004).
34. Turk, M.J. *et al.* Concomitant tumor immunity to a poorly immunogenic melanoma is prevented by regulatory T cells. *J. Exp. Med.* **200**, 771–782 (2004).
35. Alonzi, T. *et al.* Induced somatic inactivation of STAT3 in mice triggers the development of a fulminant form of enterocolitis. *Cytokine* **26**, 45–56 (2004).
36. Turkson, J. *et al.* Inhibition of constitutive Stat3 activation by novel platinum complexes with potent anti-tumor activity. *Mol. Cancer Ther.* **3**, 1533–1542 (2004).
37. Shen, Y., Devgan, G., Darnell, J.E., Jr. & Bromberg, J.F. Constitutively activated Stat3 protects fibroblasts from serum withdrawal and UV-induced apoptosis and antagonizes the proapoptotic effects of activated Stat1. *Proc. Natl. Acad. Sci. USA* **98**, 1543–1548 (2001).
38. Costa-Pereira, A.P. *et al.* Mutational switch of an IL-6 response to an interferon-gamma-like response. *Proc. Natl. Acad. Sci. USA* **99**, 8043–8047 (2002).
39. Bromberg, J. & Darnell, J.E., Jr. The role of STATs in transcriptional control and their impact on cellular function. *Oncogene* **19**, 2468–2473 (2000).
40. Yu, H. & Jove, R. The STATs of cancer–new molecular targets come of age. *Nat. Rev. Cancer* **4**, 97–105 (2004).
41. Niu, G. *et al.* Gene therapy with dominant-negative Stat3 suppresses growth of the murine melanoma B16 tumor *in vivo*. *Cancer Res.* **59**, 5059–5063 (1999).
42. Chiarle, R. *et al.* Stat3 is required for ALK-mediated lymphomagenesis and provides a possible therapeutic target. *Nat. Med.* **11**, 623–629 (2005).
43. Welte, T. *et al.* STAT3 deletion during hematopoiesis causes Crohn's disease-like pathogenesis and lethality: a critical role of STAT3 in innate immunity. *Proc. Natl. Acad. Sci. USA* **100**, 1879–1884 (2003).
44. Wang, J.W. *et al.* Influence of SHIP on the NK repertoire and allogeneic bone marrow transplantation. *Science* **295**, 2094–2097 (2002).
45. Furumoto, K. *et al.* Spleen-derived dendritic cells engineered to enhance interleukin-12 production elicit therapeutic antitumor immune responses. *Int. J. Cancer* **87**, 665–672 (2000).
46. Wei, S. *et al.* Control of lytic function by mitogen-activated protein kinase/extracellular regulatory kinase 2 (ERK2) in a human natural killer cell line: identification of perforin and granzyme B mobilization by functional ERK2. *J. Exp. Med.* **187**, 1753–1765 (1998).